

In Situ Evaluation of the LWA Analog Signal Path

Joe Craig* Steve Ellingson† Paul S. Ray‡

March 30, 2009

Contents

1	Introduction	2
2	System Description & Methodology	2
3	ARX Output	6
4	Confirmation of Galactic Noise-Limited Operation	8
A	Galactic Noise Temperature	10

*University of New Mexico, 1009 Bradbury, Albuquerque, NM 87131 USA. E-mail: joeccraig@unm.edu

†Bradley Dept. of Electrical & Computer Engineering, 302 Whittemore Hall, Virginia Polytechnic Institute & State University, Blacksburg VA 24061 USA. E-mail: ellingson@vt.edu

‡Naval Research Laboratory. E-mail: Paul.Ray@nrl.navy.mil

1 Introduction

This report documents *in situ* evaluation of the analog signal path for the Long Wavelength Array (LWA), December 19 & 20, 2008.

2 System Description & Methodology

The measurement system is diagramed in Figure 1. The signal path under test consists of the following components:

- *Antenna*: The Antenna used was the Burns Prototype fielded in Sept., 2008. The east-west oriented dipole was used for these measurements. The design of the Burns Antenna is documented in [6]. For the purposes of this testing, the antenna is conveniently characterized using the methodology in [2], and [3]. In this approach, the antenna is described in terms of its impedance mismatch efficiency (IME), which is defined as $1 - |\Gamma|^2$, where Γ is the reflection coefficient at the interface between the dipole and (in this case) a 100Ω active balun input impedance. In effect, IME is the fraction of the available antenna temperature that is effectively delivered to the active balun. IME in this case was determined using a model for antenna terminal impedance calculated using a NEC2 model of the Burns Antenna, with the result shown in Figure 3.
- *Active Balun*: LWA Front-End Electronics (FEE) version 1.6, described in [9]. The measured transfer function of FEE 1.6 is shown in Figure 4(a).
- *Coax Cable*: The cable used was 130 m of LMR-240, wrapped in conduit above the ground. The measured transfer function of this cable is shown in Figure 4(b).
- *ARX*: The LWA Brassboard Analog Receiver (ARX), described in [4], was used as a single receiver channel. The Full Bandwidth filter configuration was evaluated. A gain control (attenuation) setting of 20 dB on attenuator 1 and 20 dB on attenuator 2 was configured for present RFI levels at the LWDA site. The measured transfer function for this gain setting is shown in Figure 4(c). The ARX also provides a bias-T for powering the FEE. The bias-T design details are documented in [7].
- *DIG*: The Prototype ADC, described in [8] was configured for use with the Analog Devices, Inc. HSC-ADC-EVALC digital capture board. A clock signal of 200 MHz was applied to sample the analog signal at 200 MSPS, 12 Bits. The digital capture board interfaces to a PC via USB and bursts coherent time data at a rate of about 0.1 ms per second.
- *Digital Spectrometer*: Software, written in LabVIEW, reads the captured time data files and performs the FFT (no windowing) and integration over the full bandwidth. The digital spectrometer software automatically saves integrated spectra at the time intervals specified (approximately 1 second of full bandwidth integrated data, every half hour). A screenshot of the spectrometer software is shown in Figure 6.

The total transfer function including active balun, coax, and ARX results shown above is presented in Figure 4(d). The passband calibration used, also illustrated in figure 4(d), is given by:

$$G_{dB} = 62 - 85 \cdot 10^{-9} \times f_{Hz} \quad (1)$$

The total calibrated transfer function is shown in Figure 5. The same result, including IME is also shown. This result is the expected transfer function from antenna temperature (nominally dominated by Galactic noise) to ARX output.

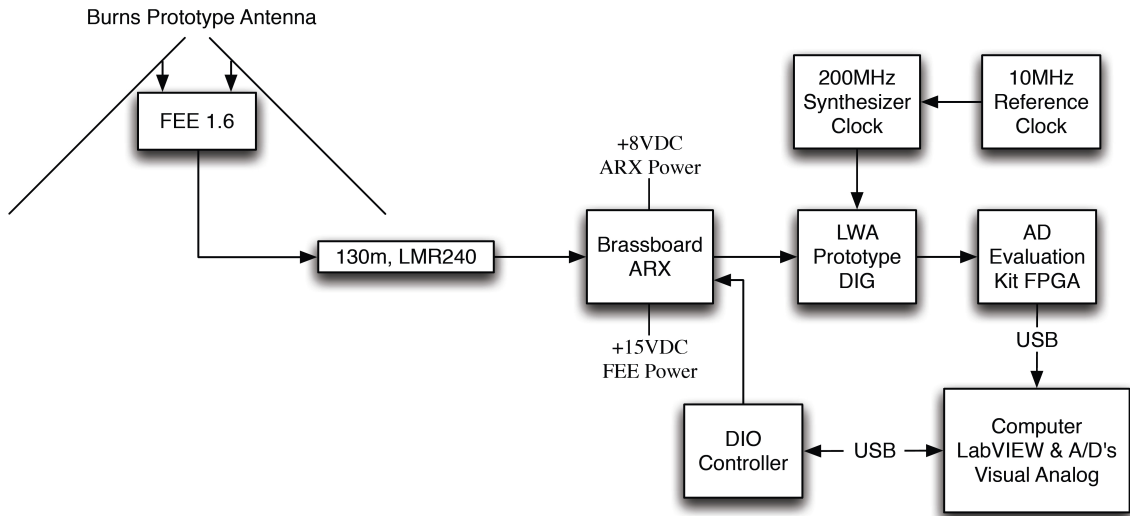


Figure 1: System diagram of setup used for signal path evaluation.

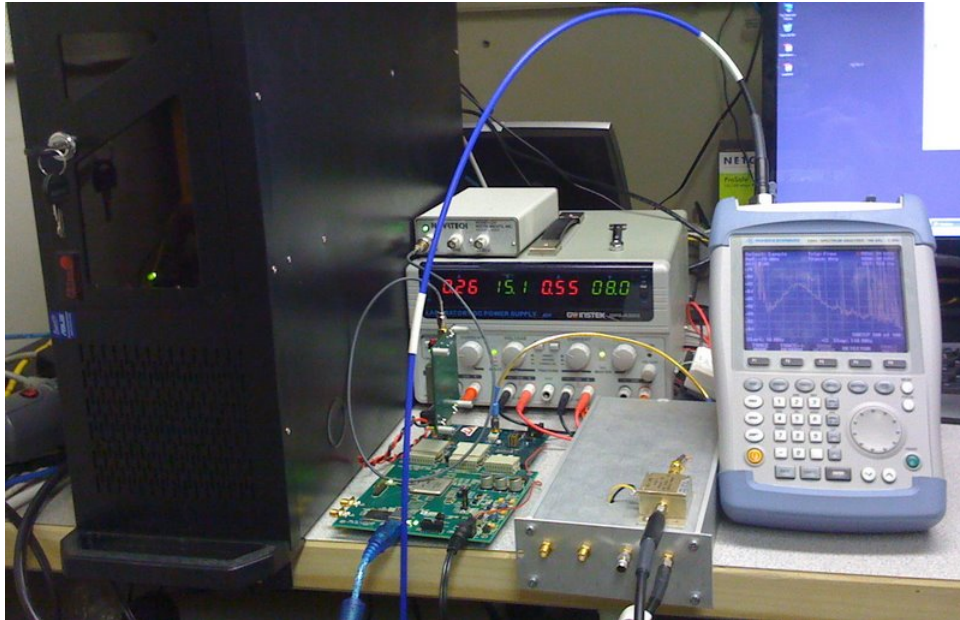


Figure 2: Photo of the hardware used in this evaluation.

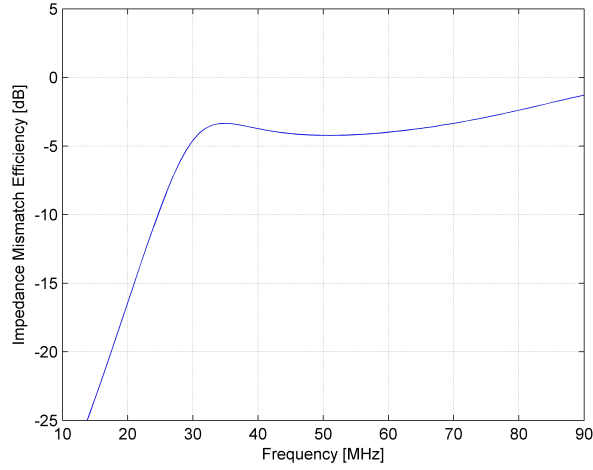
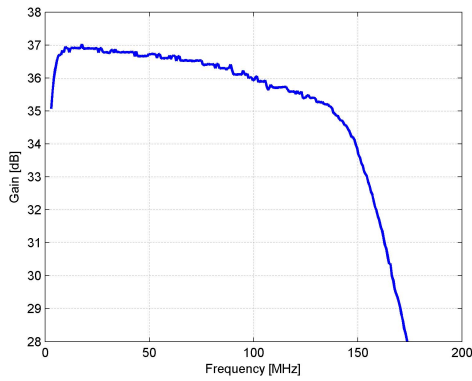
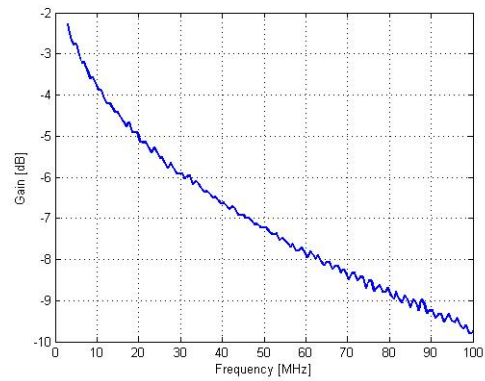


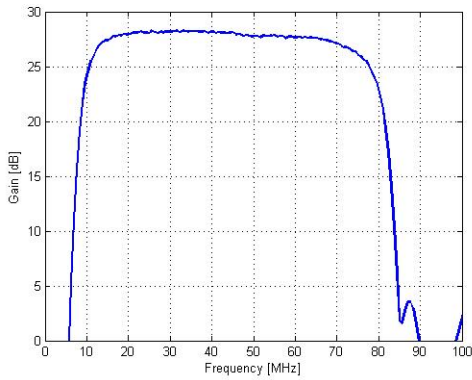
Figure 3: IME of Burns Prototype antenna connected a 100Ω active balun input impedance, determined using terminal impedance calculations from a NEC2 model.



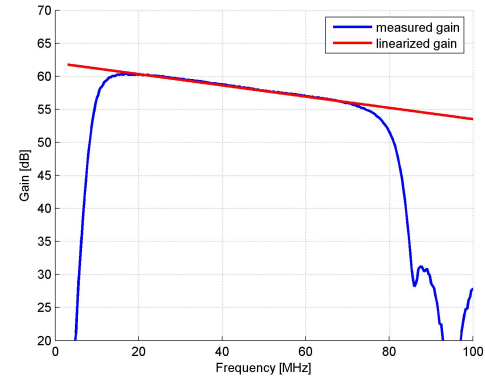
(a) Active Balun, FEE 1.6



(b) Coaxial Cable, 130 m of LMR-240



(c) Analog Receiver, Brassbord ARX in Full Bandwidth filter configuration.



(d) Entire Receive Chain. *Blue Line*: Measured transfer function. *Red Line*: Linearized transfer function (1) applied for calibration.

Figure 4: Measured Transfer Function of the Receiver Components.

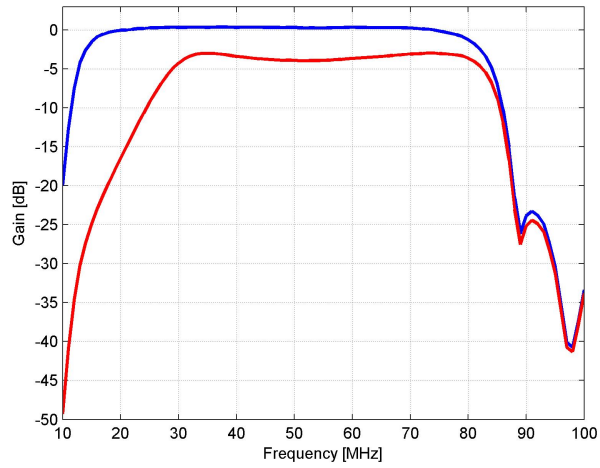


Figure 5: *Blue Line*: The measured total transfer function with passband calibration applied. *Red Line*: Same, except now including the antenna response (IME) from antenna simulations.

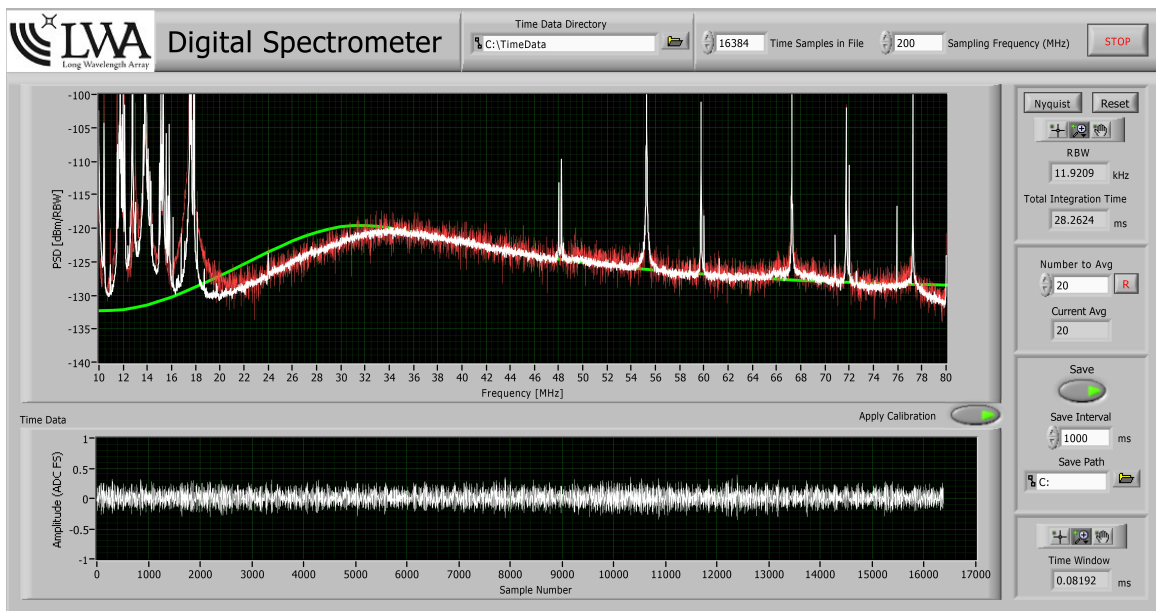


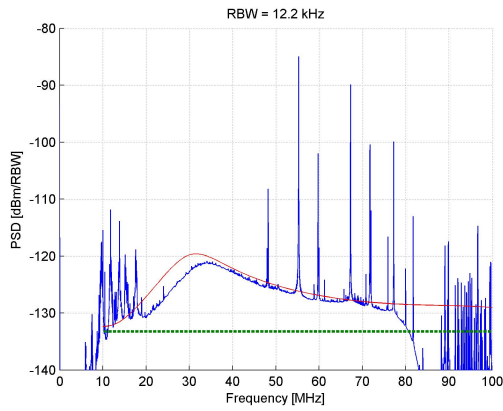
Figure 6: Screenshot of the digital spectrometer software. The lower portion displays a time-domain window of $81.92 \mu\text{s}$. The frequency response shows the integrated power spectral density in white and the current time-window's spectral density in red. The model sky temperature (with antenna IME) is shown in green.

3 ARX Output

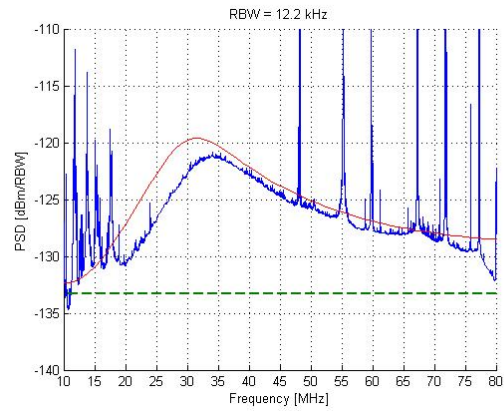
Figure 7(a) & 7(b) show the output of the ARX, measured over a period of about 48 contiguous hours. The similarity to Figure 5 is apparent. Also apparent is strong RFI corresponding to TV stations, HF communications, and FM radio stations. Note, the FM stations have been suppressed significantly by the ARX.

Figure 8 shows the same result, but now calibrated to remove the ARX, coax, active balun, and antenna (IME). Thus, this represents power actually incident on the antenna. Clearly visible is a slope in the noise floor attributable to the Galactic background.

Figures 9 & 10 show the same data as in Figures 7(b) & 8, but now in the form of dynamic spectra. The diurnal variation of the antenna temperature is clearly visible.



(a) Output of Digital Spectrometer



(b) Same, zoomed into the passband.

Figure 7: *Blue Line*: Mean value after 2 days of continuous measurements. The frequency response has been calibrated by (1). *Red Line*: Sky Temperature Model with Antenna IME. *Green/Dashed Line*: Receiver Temperature.

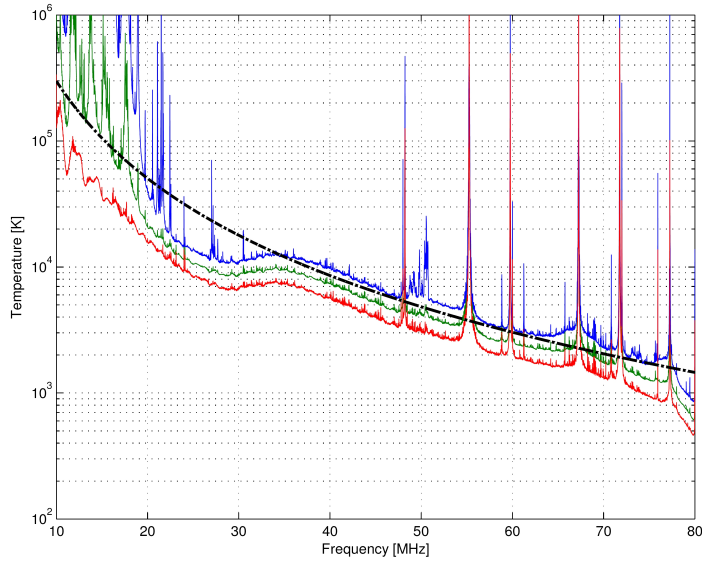


Figure 8: Measured temperature (max, mean, min) & the model Galactic background temperature (see Appendix A). The deviation from the sky model at frequencies below 35 MHz may be due to the variation in antenna impedance from the modeled IME.

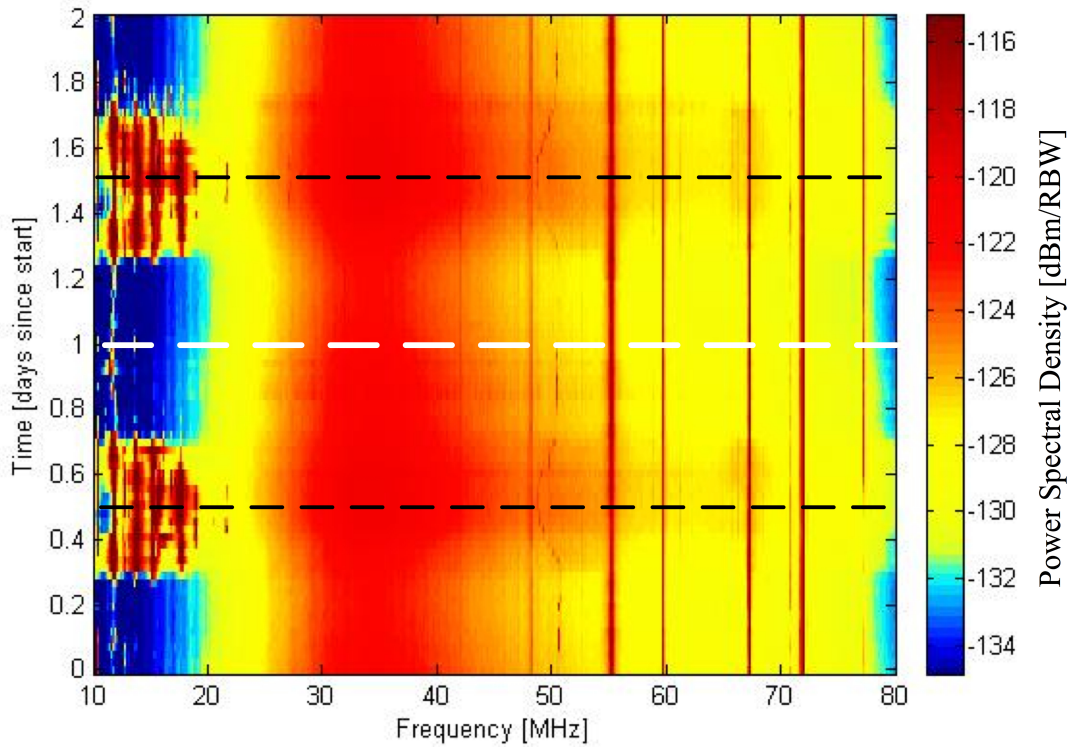


Figure 9: Dynamic spectra from 2 day measurements. Black dotted line corresponds to local Galactic maximum and the white dotted line is Galactic minimum. Time = 0 corresponds to midnight, MST (7:00 AM UTC). Power levels are calibrated per (1). Note that during the daytime, the 10 MHz to 20 MHz (HF Communications) RFI levels peak up drastically as compared to the nighttime.

4 Confirmation of Galactic Noise-Limited Operation

Figure 10 shows the total power in a 1 MHz bandwidth at 4 frequencies, after calibration to remove all instrumental responses. Diurnal variation is clearly visible. Note that there is no flattening around the daily minimums, which would indicate that internally-generated noise was starting to dominate. Also note that the variation at the highest frequency appears to be the same as the variation at lower frequencies, suggesting that the system is strongly Galactic noise-limited throughout the passband.

LFmap, a low-frequency sky map [12] program was used to create the expected drift curve at 46 MHz. The model data is plotted along with the measured data in figure 11. The diurnal variations clearly follows the shape of the modeled data, indicating the receiver is Galactic noise dominated.

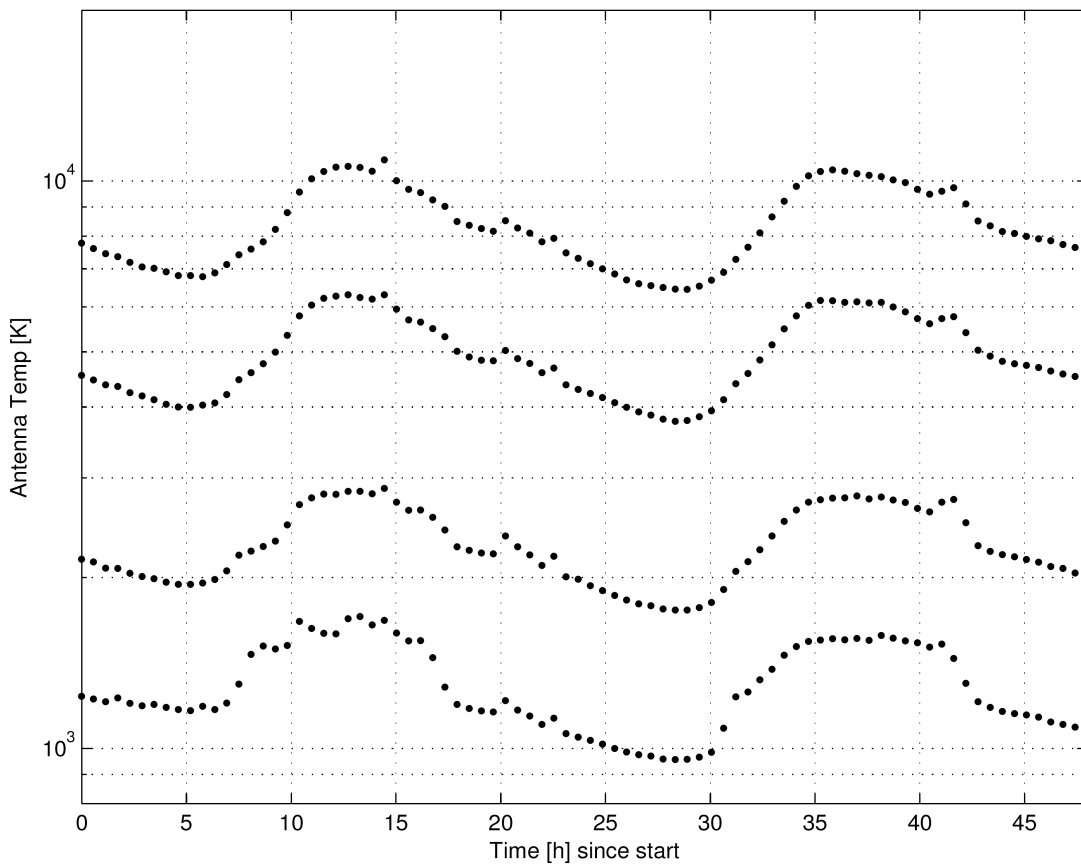


Figure 10: Total Power measured over a 1 MHz bandwidth at four frequencies. *Top to Bottom*: 38 MHz, 46 MHz, 63 MHz, 75 MHz

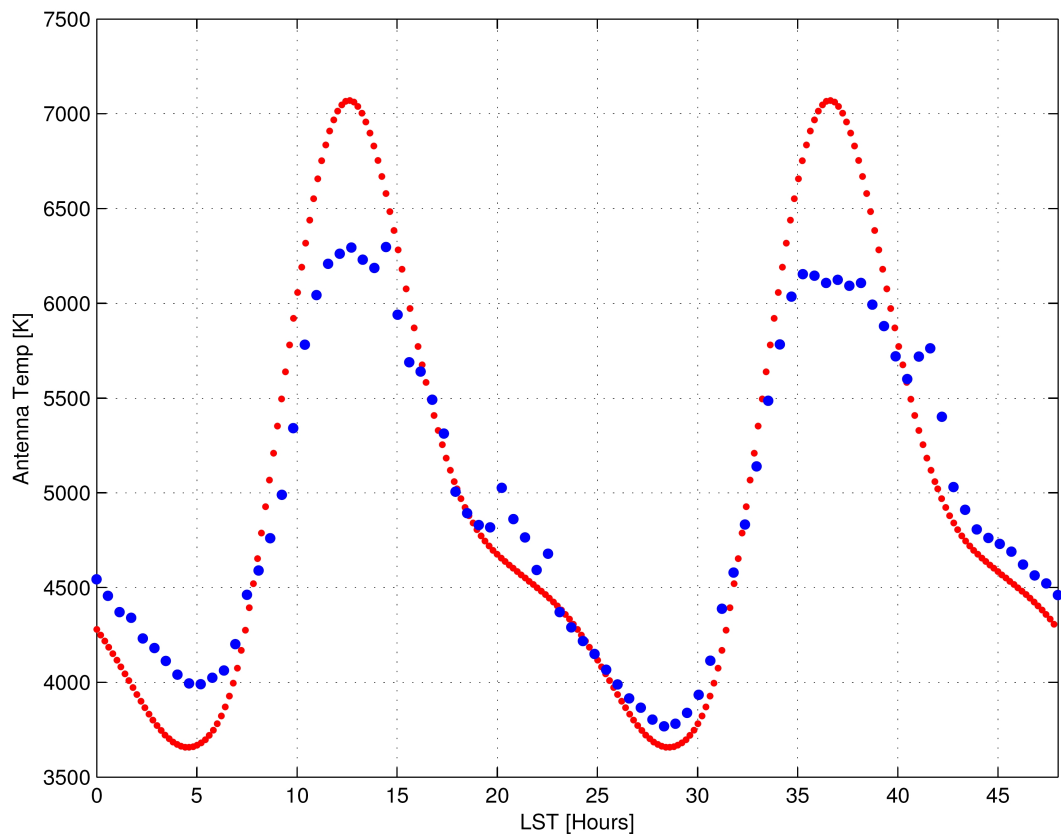


Figure 11: *Blue Points*: Measured total power at antenna terminals at 46 MHz. *Red Points*: LFmap model sky temperature at 46 MHz.

References

- [1] J. Craig, S.W. Ellingson, “Laboratory Measurements of the Brassboard ARX,” LWA Engineering Memo ARX0014, October 9, 2008. <http://panda.unm.edu/lwa/engineering>.
- [2] S. Ellingson, “*In Situ* Evaluation of the ETA Analog Signal Path,” LWA Memo 46, Aug 11, 2006. <http://www.ece.vt.edu/swe/lwa/>
- [3] S. Ellingson, J. Simonetti, and C. Patterson, “Design and Evaluation of an Active Antenna for a 29-47 MHz Radio Telescope Array,” LWA Memo 60, *IEEE Trans. Ant. and Prop.*, Vol 55, No. 3, March 2007, pp 826-831. <http://www.ece.vt.edu/swe/lwa/>
- [4] J. Craig, “ARX Strawman Design,” LWA Engineering Memo ARX0004A, May 1, 2008. <http://panda.unm.edu/lwa/engineering>.
- [5] P.S. Ray, *et al.*, “Specifications of the GASE Antennas,” LWA Memo 40, June 14, 2006. <http://www.ece.vt.edu/swe/lwa/>.
- [6] N. Paravastu, “Antenna Design for LWA-1,” LWA Engineering Memo ANT0007, Aug 29, 2008. <http://panda.unm.edu/lwa/engineering>.
- [7] B. Hicks, B. Erickson, “Bias-T Design Considerations for the LWA,” LWA Memo 135, Apr 29 2008. <http://www.ece.vt.edu/swe/lwa/>
- [8] M. Harun, S. Ellingson, “Design and Development of a Prototype ADC for LWA,” LWA Memo 127, Mar 4 2008. <http://www.ece.vt.edu/swe/lwa/>
- [9] B. Hicks, N. Paravastu, “The Rapid Test Array Balun (G250R),” LWA Memo 120, Dec 12 2007. <http://www.ece.vt.edu/swe/lwa/>
- [10] S.W. Ellingson, “Antennas for the Next Generation of Low Frequency Radio Telescopes,” LWA Memo 22, August 2005. <http://www.ece.vt.edu/swe/lwa/>
- [11] H. V. Cane, ”Spectra of the nonthermal radio radiation from the Galactic polar regions,” Monthly Notice Royal Astronomical Society, vol. 189, p. 465, 1979
- [12] E. Polisensky, “LFmap: A Low Frequency Sky Map Generating Program,” LWA Memo 111, Sept 7, 2007. <http://www.ece.vt.edu/swe/lwa/>

A Galactic Noise Temperature

As in [5] and [10], we need to understand the noise power incident on the antenna as it relates to the Galactic noise temperature. If we assume the the system temperature is effectively dominated by Galactic noise,

$$T_{sky} = \frac{I_{\nu} c^2}{2 k \nu^2} \quad (2)$$

where $k = 1.38 \times 10^{38}$ J/K is Boltzmann’s constant, c is the speed of light, ν is the frequency in Hz, and I_{ν} is the intensity of Galactic noise in $\text{W m}^{-2} \text{Hz}^{-1} \text{sr}^{-1}$. Following [10], [5], and [11], we can approximate I_{ν} by,

$$I_{\nu} \approx I_g \nu^{-0.52} + I_{eg} \nu^{-0.80} \quad (3)$$

where $I_g = 2.48 \times 10^{-20}$ is the noise contribution by Galactic sources, and $I_{eg} = 1.06 \times 10^{-20}$ is the noise contribution by extra-Galactic sources. The result is shown as the dashed line in figure 8.